Hic-5 antisense oligonucleotide inhibits advanced hepatic fibrosis and steatosis *in vivo*
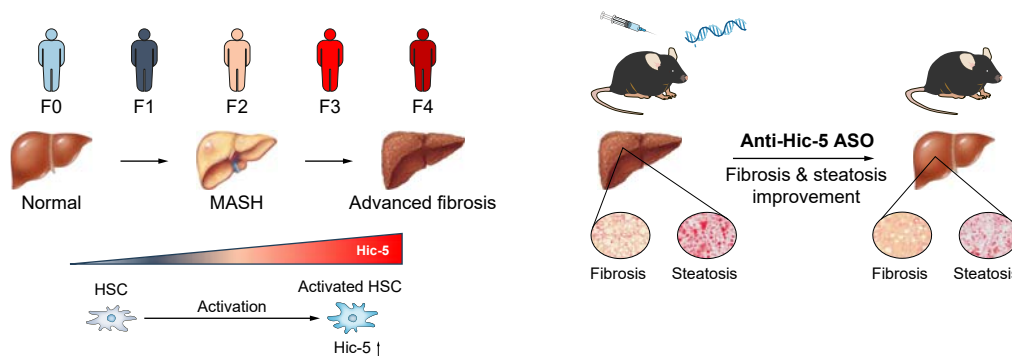
Authors

Masahito Noguchi, Aya Miyauchi, Yoshiaki Masaki, …, Hitoshi Yoshida, Kohji Seio, Joo-ri Kim-Kaneyama

Correspondence

kseio@bio.titech.ac.jp (K. Seio), shuri@pharm.showa-u.ac.jp (JR. Kim-Kaneyama).

Graphical abstract

Highlights:

- Liver fibrosis was ameliorated by inhibiting a single adaptor molecule.

- The pathogenesis of liver fibrosis and steatosis was controlled by anti-*Hic-5* ASO.

- Anti-*Hic-5* ASO designed in this study is a clinically applicable therapeutic modality.

Impact and implications:

This study investigated the role of Hic-5 in liver fibrosis and steatohepatitis, highlighting its potential as a therapeutic target. We developed an antisense oligonucleotide (ASO) that was particularly transportable to the liver, and targeted Hic-5. Anti-*Hic-5* ASO exhibited therapeutic efficacy for liver fibrosis and steatosis *in vivo*, indicating its therapeutic potential for liver fibrosis and steatosis. ASOs have already achieved dramatic therapeutic effects as approved nucleic acid drugs. Thus, anti-*Hic-5* ASO is expected to lead the direct generation of seed compounds for the clinical development of drugs for liver fibrosis and steatosis.

Hic-5 antisense oligonucleotide inhibits advanced hepatic fibrosis and steatosis *in vivo*

Masahito Noguchi[1,†], Aya Miyauchi[1,2,†], Yoshiaki Masaki[3,†], Masashi Sakaki[4], Xiao-Feng Lei[5], Momoko Kobayashi-Tanabe[1], Akira Miyazaki[1,2], Takeshi Aoki[6], Hitoshi Yoshida[4], Kohji Seio[3,*,‡], Joo-ri Kim-Kaneyama[1,2,*,‡]

Check for updates

Background & Aims: Chronic liver diseases, including metabolic dysfunction-associated steatohepatitis (MASH), pose a significant global health burden. Progressive liver fibrosis can lead to severe outcomes; however, there is a lack of effective therapies targeting advanced fibrosis. Hydrogen peroxide-inducible clone-5 (Hic-5), an adaptor protein in focal adhesion, is critical for promoting liver fibrosis in hepatic stellate cells. This study investigated its clinical applicability by examining hepatic Hic-5 expression in human fibrotic tissues, exploring its association with MASH, and assessing the therapeutic potential of antisense oligonucleotides (ASOs) targeting Hic-5 in a MASH mouse model.

Methods: Hepatic Hic-5 expression in human fibrotic tissues underwent pathological image analysis and single-cell RNA sequencing. ASOs targeting Hic-5 were developed and tested using *in vitro* cell models. An *in vivo* MASH mouse model was used to evaluate the effects of anti-*Hic-5* ASOs on advanced fibrosis and steatosis.

Results: Hepatic Hic-5 expression increased with the progression of fibrosis, particularly in advanced stages. Single-cell RNA sequencing revealed Hic-5 expression primarily in hepatic stellate cells. In MASH-associated fibrosis, Hic-5 expression correlated with the expression of fibrotic genes. In the MASH mouse model, hepatic Hic-5 expression increased with disease progression. Anti-*Hic-5* ASOs effectively suppressed Hic-5 expression *in vitro* and attenuated advanced fibrosis and steatosis *in vivo*, indicating their therapeutic potential.

Conclusions: Hepatic Hic-5 expression is associated with advanced liver fibrosis and MASH. Anti-*Hic-5* ASOs are promising therapeutic interventions for MASH accompanied by advanced fibrosis. These findings provide valuable insights into potential clinical treatments for advanced liver fibrosis.

Introduction

Metabolic dysfunction-associated steatotic liver disease (MASLD), formerly known as non-alcoholic fatty liver disease, has rapidly become the most common liver disease globally and is currently estimated to affect 38% of the population.[1] Fibrosis stage, but not other histological characteristics, predicts overall mortality in MASLD.[2] Untreated liver fibrosis can lead to hepatic cirrhosis, life-threatening liver failure, and hepatocellular carcinoma. However, there is no effective therapy that directly targets and reverses advanced fibrosis except removal of the underlying etiology or liver transplantation.[3–6] Therefore, a new therapeutic approach to reverse liver fibrosis is needed.

Although liver fibrosis, characterized by the deposition of connective tissue, is a reversible wound healing process after liver injury, chronic liver diseases caused by viral infection, chronic ethanol consumption, metabolic disorders, or autoimmune imbalances lead to the irreversible and excessive accumulation of extracellular matrix (ECM) and impaired liver function.[7] Excessive accumulation of ECM during liver fibrosis increases stiffness, adding mechanical stress to ECM-producing cells, increasing collagen production and collagen crosslinking, leading to fibrosis, which is part of ECM remodeling. The regulation of ECM remodeling is considered a key to fibrosis therapy.

Hydrogen peroxide-inducible clone-5 (Hic-5), a focal adhesion adaptor protein whose gene is induced by hydrogen peroxide and transforming growth factor (TGF)-β1,[8] has a role in regulating ECM remodeling in various diseases.[9] Previously, we observed a marked elevation in Hic-5 expression within the stromal microenvironment of human colorectal cancer. Hic-5 expression levels had a significant positive correlation with ESTIMATE-based stromal scores, indicators of stromal abundance within the tumor milieu, across four distinct colorectal cancer datasets. Additionally, stromal Hic-5 regulates cancer cell proliferation and

lysyl oxidase (LOX) expression in cancer-associated fibroblasts. In a murine model of azoxymethane-induced colorectal cancer, the incidence of tumor development was suppressed in Hic-5 deficient mice relative to wild-type (WT) mice, indicating the critical role of Hic-5 in the context of cancer characterized by desmoplastic stroma. In the liver, Hic-5 is mainly expressed in hepatic stellate cells (HSCs), major precursors of activated myofibroblasts that produce ECM proteins during liver fibrosis.[10,11] We previously reported Hic-5 expression was higher in fibrotic human livers compared with normal livers and that liver fibrosis induced by CCl$_4$ injection and bile duct ligation was attenuated in Hic-5-deficient mice.[10] Moreover, Hic-5 knockdown using small interfering RNA (siRNA) repressed murine liver fibrosis caused by CCl$_4$, suggesting Hic-5 is a promising therapeutic target for liver fibrosis.[10]

siRNA specifically targets intracellular molecules, such as Hic-5. However, naked siRNA is easily degraded by nucleases in the blood, leading to poor accumulation in target tissues. Thus, drug delivery systems such as lipid nanoparticles are required to carry siRNA to the target tissue. In contrast, antisense oligonucleotide (ASO), a nucleic acid-based medicine similar to siRNA, is preferentially delivered to the liver by subcutaneous injection. We hypothesized anti-*Hic-5* ASOs would be suitable for the clinical treatment of liver fibrosis. This study investigated the therapeutic efficacy of anti-*Hic-5* ASO, which might aid the development of liver fibrosis drugs.

Materials and methods

Please refer to the Supplementary materials and methods for more detailed descriptions. Antibodies, ASO sequences and primers used in this study were listed in Supplementary Table S2-S4.

Human liver specimens

Sections from livers in fibrosis stages F0 (n = 11), F1 (n = 12), F2 (n = 13), F3 (n = 10), and F4 (n = 8) were obtained from hepatocellular carcinoma patients undergoing surgical hepatectomy at Showa University Hospital. This study used non-cancerous lesions from these livers. Liver fibrosis stage was determined at the Department of Pathology and Laboratory Medicine, Showa University School of Medicine. The study protocol was approved by the Ethics Committee of Showa University School of Medicine, Tokyo, Japan. We applied an opt-out method to obtain patient consent.

Animal experiments

All animal experiments followed the study protocol approved by the Ethics Committee of Showa University School of Medicine. In intervention studies (siRNA or ASO treatment), we established safety laboratory parameters, including rapid weight loss and injection site reactions. Experiments would be halted if a 20% body weight loss within 1 week or symptoms of suppuration at the injection site occurred. None of these phenomena were observed in the study. All methods were reported in accordance with ARRIVE guidelines (https://arriveguidelines. org). Male WT C57/BL6N mice were obtained from Sankyo Lab Service Co. (Tokyo, Japan). Metabolic dysfunction-associated steatohepatitis (MASH) model mice were induced by feeding them a choline-deficient, L-amino acid-defined,

high-fat diet (CDAHFD) (A06071302; Research Diets Inc., NJ, USA). Mice in the standard-chow diet group were fed PicoLab Mouse Diet 20 (5058; Land O'Lakes Inc., MN, USA) for 6 weeks. WT and systemic Hic-5 knockout (KO) mice (C57BL/6 background) were housed under specific pathogen-free conditions in the animal care facility of Showa University School of Medicine.[12]

Statistical analysis

Unpaired two-tailed t tests were used to compare two groups of samples. One-way ANOVA with Dunnett's multiple comparison test or Tukey's multiple comparison test was used to compare data from more than three groups. Data are presented as the mean ± SEM. Values of $p < 0.05$ were considered significant. All analyses were performed using GraphPad Prism software (GraphPad Software, San Diego, CA, USA).

Results

Hepatic Hic-5 expression is increased in patients with advanced liver fibrosis

To elucidate alterations in Hic-5 expression throughout the progression of fibrosis in humans, we analyzed 54 liver sections from patients with different pathological fibrosis stages (F0–F4; Fig. 1A, Fig. S1). Clinical characteristics and features of patients are summarized in Table S1. Among 12 patients with HBV, nucleotide analog therapy for viral control was administered to three patients during surgical procedures. The remaining cases were past infections where the virus had been rendered undetectable. In addition, there were 18 patients with HCV in this study, with the status unknown in three, and one where the virus was still present. The other 14 patients achieved viral clearance following treatment. Image analysis identified a greater area of Hic-5-positive tissue in patients with advanced fibrosis (stages F3, F4) compared with stages F0 and F1 (Fig. 1B). Fibrosis areas quantified using Masson's trichrome staining indicated a robust positive correlation between Hic-5-positive areas and extent of fibrosis (Fig. 1C). Furthermore, Hic-5 fluorescence intensities were significantly higher in patients at stages F3 and F4 compared with stage F0 (Fig. 1D and E). Analysis of Hic-5 fluorescence intensity and fibrosis area identified a positive correlation (Fig. 1F). These data demonstrate a positive correlation between Hic-5 expression and hepatic fibrosis progression in humans. Notably, Hic-5 is significantly upregulated at advanced fibrosis stages F3–F4.

Human hepatic *HIC-5* is mainly expressed in mesenchymal cells

To analyze the expression and localization of *HIC-5* within cirrhotic livers, we used a public single-cell RNA sequencing (scRNA-seq) dataset (GSE136103). scRNA-seq analysis indicated *HIC-5* was expressed in mesenchymal cells, and especially in HSCs and smooth muscle cells (Fig. 2A). A previous study reported Hic-5 expression in HSCs and vascular smooth muscle cells (VSMCs) of Glisson's sheath in normal liver.[10] Fibrotic genes encoding collagen type I alpha 1 chain (*COL1A1*) and collagen type I alpha 2 chain (*COL1A2*) are also expressed in mesenchymal cells, especially HSCs (Figs. S2A and B). Focusing on the cluster of HSCs, patients with cirrhosis had a greater proportion of *HIC-5*-positive cells than
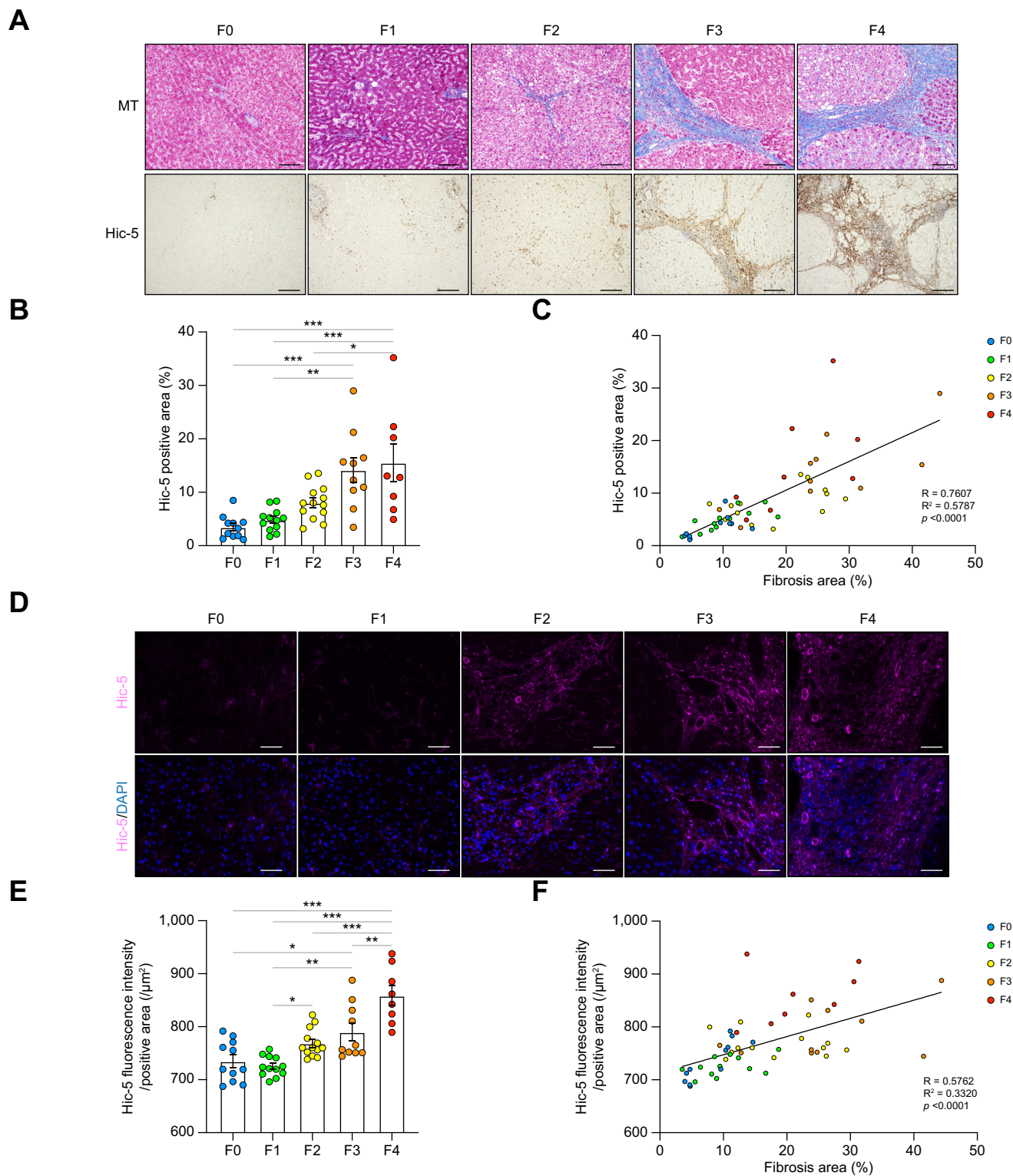
Fig. 1. Hic-5 expression increases with human liver fibrosis progression. (A) Representative images of Hic-5 and Masson's trichrome (MT) staining of human liver (fibrosis stages F0/F1/F2/F3/F4: n = 11/12/13/10/8). Scale bars: 200 μm. (B) Hic-5-positive areas in patient livers with fibrosis. (C) Linear correlation between fibrosis area and Hic-5-positive area (*R*, Pearson's coefficient). (D) Representative immunofluorescence images of Hic-5 (magenta). Nuclei were stained with DAPI. Scale bars: 50 μm. (E) Hic-5 fluorescence intensity per unit Hic-5-positive area. (F) Linear correlation between fibrosis area and Hic-5 fluorescence intensity per unit Hic-5-positive area. Values are means ± SEM. *p <0.05, **p <0.01, ***p <0.001, Tukey's multiple comparison test (B, E).
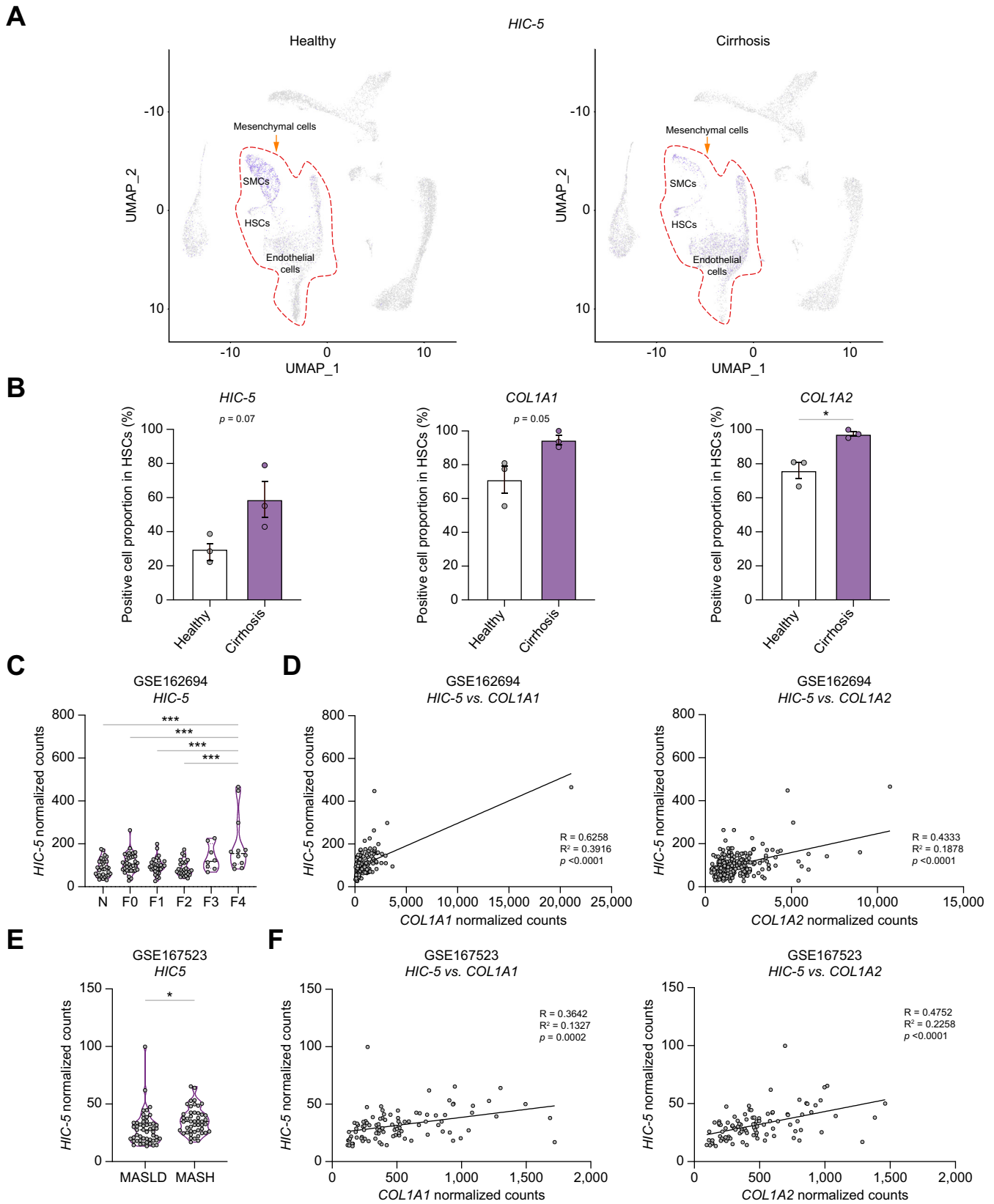
Fig. 2. HIC-5 is associated with MASLD progression. (A) *HIC-5* in healthy and cirrhotic human liver cells. Dashed lines indicate mesenchymal cell clusters. (B) HSCs expressing *HIC-5, COL1A1,* and *COL1A2* in healthy and cirrhotic livers (n = 3/group). (C) *HIC-5* in livers of healthy individuals and MASLD with fibrosis (N/F0/F1/F2/F3/F4: n = 31/35/30/27/8/12). N: Healthy. (D) Linear correlation between *HIC-5* and *COL1A1* and between *HIC-5* and *COL1A2*. (E) *HIC-5* in livers of patients with MASLD and MASH (MASLD/MASH: n = 47/51). (F) Linear correlation between *HIC-5* and *COL1A1* and between *HIC-5* and *COL1A2*. Values are mean ± SEM. *p <0.05, ***p <0.001, two-tailed Student's t test (B) and Tukey's multiple comparison test (C, E). HSCs, hepatic stellate cells; MASH, metabolic dysfunction-associated steatohepatitis; MASLD, metabolic dysfunction-associated steatotic liver disease; SMCs, smooth muscle cells.

healthy controls, and a similar observation was made for *COL1A1*-and *COL1A2*-positive cell proportions (Fig. 2B). Thus, Hic-5 in HSCs is associated with fibrosis progression.

HIC-5 is associated with MASLD progression

We investigated human hepatic *HIC-5* expression using public bulk RNA-seq datasets GSE162694 and GSE167523. Dataset GSE162694 was acquired using 143 adult liver tissues with MASLD and all stages of fibrosis, and GSE167523 was acquired using 98 adult liver tissues with MASLD.[13,14] The raw gene count matrixes of these datasets were obtained from the Gene Expression Omnibus and normalized relative to the count matrixes obtained using the DEseq2 method.[15] Normalized count data indicated *HIC-5* expression was significantly increased in F4 with MASLD (Fig. 2C). Positive correlations were identified between *HIC-5* and *COL1A1* expressions, and between *HIC-5* and *COL1A2* expressions (Fig. 2D). *HIC-5* expression levels were significantly higher in patients with MASH compared with MASLD (Fig. 2E), indicating *HIC-5* expression was correlated with *COL1A1* and *COL1A2* expression levels (Fig. 2F) suggesting *HIC-5* is associated with fibrotic genes in MASH.

Hic-5 expression is enhanced in a diet-induced MASH mouse model

To investigate Hic-5 expression in MASLD progression, we generated a mouse MASH model induced by feeding mice a CDAHFD. In this model, a time-dependent increase in fibrosis was observed during 6 weeks of feeding.[16] Pathological fibrosis in mice fed a CDAHFD for 6–15 weeks was observed, and fibrosis areas were measured by Sirius Red (SR) staining (Fig. 3A and B). Steatosis was observed after 3 weeks of feeding and steatosis levels were measured based on the area of Oil Red O staining (Fig. 3A and C). Quantitative real-time reverse transcriptase PCR (qPCR) analysis confirmed hepatic *Hic-5* expression was markedly increased after 3 weeks of feeding (Fig. 3A and D). *Col1a1* and *Col1a2* expressions were increased after 3 weeks of feeding. Furthermore, *Hic-5* expression positively correlated with *Col1a1* and *Col1a2* expressions (Fig. 3E and F). Similar to human transcriptomic data, *Hic-5* mRNA expression was significantly higher in MASH mice.

Hic-5 deficiency reduces CDAHFD-induced hepatic fibrosis in mice

To investigate Hic-5 in MASH-associated fibrosis, we induced liver fibrosis using a CDAHFD in WT and Hic-5 KO mice. The role of Hic-5 at the early onset of MASH and during chronic MASH was analyzed using feeding regimens of 6 and 53 weeks, respectively. After feeding with a CDAHFD, the fibrosis area (SR staining) in Hic-5 KO mice was significantly smaller than in WT mice after 6 and 53 weeks of feeding (Fig. 4A and B). Although Hic-5 was not localized to parenchymal cells, Oil Red O-stained liver sections indicated significantly less steatosis in Hic-5 KO mice than in WT mice, after 6 and 53 weeks of feeding with CDAHFD (Fig. 4A and C). Hepatic inflammation assessed by immunostaining of ionized calcium-binding adaptor molecule 1 (Iba1), a macrophage marker indicated no difference compared with WT mice (Figs. S3A and B). Liver injuries assessed by plasma concentrations of aspartate aminotransferase (AST) and alanine aminotransferase (ALT) in

Hic-5 KO mice were not significantly different from WT mice (Fig. S3C), indicating Hic-5 is involved in fibrosis and steatosis without inflammation. No macroscopic changes were observed in livers (Fig. S4A). Expression levels of *Col1a1* and *Col1a2* were higher in fibrotic livers of WT mice than Hic-5 KO mice fed CDAHFD for 6 and 53 weeks (Fig. 4D). LOX enzymes are involved in ECM remodeling via cross-linking of collagens and/or elastin. Lysyl oxidase-like 1 (LOXL1) and LOXL2 are upregulated in chronic liver disease.[17–20] Furthermore, LOX expression was induced by nuclear-localized Hic-5 in cancer-associated fibroblasts isolated from patients with colorectal cancer.[21] Therefore, we evaluated the expressions of *Lox*, *Loxl1*, and *Loxl2* in livers of mice fed CDAHFD and found no differences compared with chow-fed mice (Fig. 4E). However, *Lox* expression in 6- and 53-week CDAHFD Hic-5 KO mice was significantly lower than in WT mice (Fig. 4E). *Loxl1* and *Loxl2* expressions in Hic-5 KO mice tended to be lower than in WT mice 6 weeks after starting the CDAHFD and were significantly lower at 53 weeks (Fig. 4E). Immunohistochemical analysis indicated Hic-5 colocalized with alpha-smooth muscle actin (α-SMA), a marker of activated HSCs, indicating Hic-5 is also expressed in activated HSCs (Fig. 4F) Thus, Hic-5 might contribute to MASH-associated fibrosis and steatosis via an inflammation-independent pathway.

In vivo knockdown of Hic-5 attenuates CDAHFD-induced hepatic fibrosis and steatosis

To evaluate the therapeutic potential of Hic-5 to treat early-stage fibrosis during the onset of MASH, siRNA targeting *Hic-5* was intravenously injected through the tail vein of mice at weeks 3, 4, and 5 of CDAHFD feeding (Fig. 5A). siRNA treatment significantly decreased *Hic-5* mRNA expression (Fig. 5B and C). SR staining demonstrated the anti-fibrotic effects of Hic-5 siRNA in MASH mice (Fig. 5C), and significantly less CDAHFD-induced hepatic fibrosis was present in Hic-5 siRNA-treated mice compared with controls (Fig. 5D). Oil Red O staining indicated less steatosis in Hic-5 siRNA-treated mice compared with controls (Fig. 5C and E). Significantly less *Col1a1* and *Col1a2* mRNA was observed in Hic-5 siRNA-treated mice compared with controls (Fig. 5F). No macroscopic changes were observed in any livers (Fig. S4B). Liver injuries, assessed by measuring blood AST and ALT, were not significantly changed in Hic-5 siRNA-treated mice (Fig. S5A). Significantly less *Lox* and *Loxl2* were present in Hic-5 siRNA-treated mice compared with controls (Fig. 5G). Thus, siRNA knockdown of Hic-5 inhibited CDAHFD-induced liver fibrosis and steatosis *in vivo*, suggesting Hic-5 is a potential therapeutic target for MASH.

Design and screening of anti-*Hic-5* ASOs

We developed anti-*Hic-5* ASOs for clinical applications. To select target sites, we predicted the Hic-5 mRNA loop structures using the Mfold web server.[22] Target sites were completely common or within three miss-matches among *Homo sapiens*, *Mus musculus*, and *Rattus norvegicus* sequences, and five anti-*Hic-5* ASOs (M7, M8, H11, H13, and H26) containing locked nucleic acids (LNAs), which increase binding affinity and prevent degradation by nucleases, were designed (Fig. 6A). To verify the inhibitory effects of these ASOs on Hic-5 expression, we transfected them in human primary HSCs and mouse primary VSMCs, which highly express Hic-5.
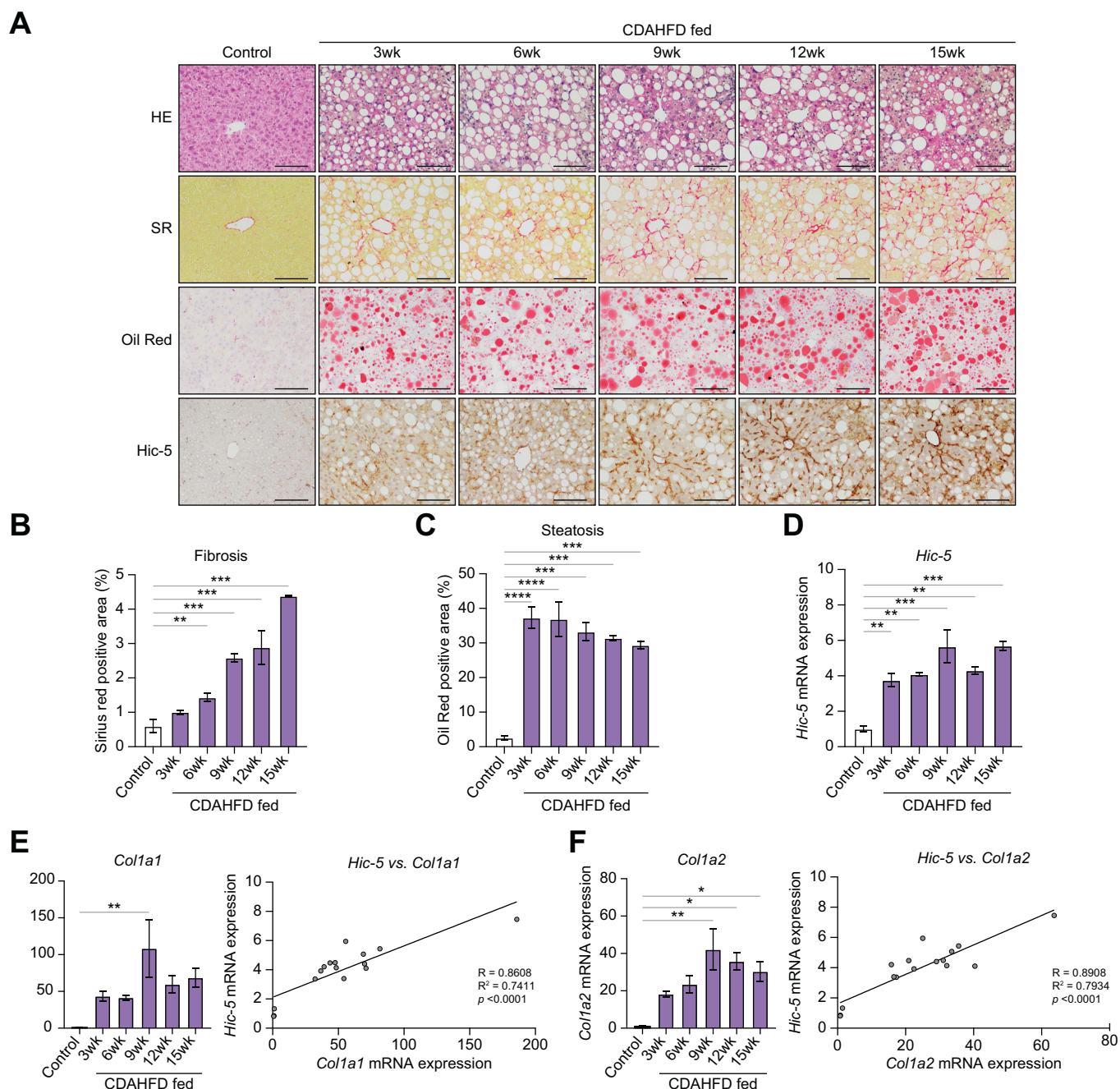
Fig. 3. Hic-5 expression in a MASH model. (A) Representative images of H&E, SR, and Oil Red O staining in livers of mice fed standard chow for 6 weeks (control) or CDAHFD for 3–15 weeks. (B) Quantitation of hepatic fibrosis. Scale bars: 200 μm (n = 2–3/group). (C) Quantitation of steatosis. (D) *Hic-5* expression. (E) *Col1a1* expression and analysis of its linear correlation with *Hic-5*. (F) *Col1a2* expression and analysis of its linear correlation with *Hic-5*. Control: mice fed standard chow for 6 weeks. Values are mean ± SEM. *p <0.05, **p <0.01, and ***p <0.001, Dunnett's multiple comparison test. CDAHFD, choline-deficient, L-amino acid-defined, high-fat diet; SR, Sirius Red.

Hic-5 expression was suppressed by all anti-*Hic-5* ASOs in human HSCs and by all ASOs except H11 in mouse VSMCs (Fig. 6B). Similarly, all five ASOs decreased Hic-5 expression in the human cell line KMST-6 and rat cell line JTC-19 (Fig. 6C). Thus, the anti-*Hic-5* ASOs suppressed Hic-5 expression in human, mouse, and rat cells. Moreover, cell viability and caspase 3/7 assays were performed to investigate ASO-induced cytotoxicity. H11 was excluded because it decreased

cell viability and induced apoptosis in NIH3T3 cells (Fig. 6D and E).

Anti-*Hic-5* ASOs decrease Hic-5 protein expression in human HSCs

Next, we examined whether anti-*Hic-5* ASOs suppressed *Hic-5* mRNA expression and protein levels. Anti-*Hic-5* ASOs reduced
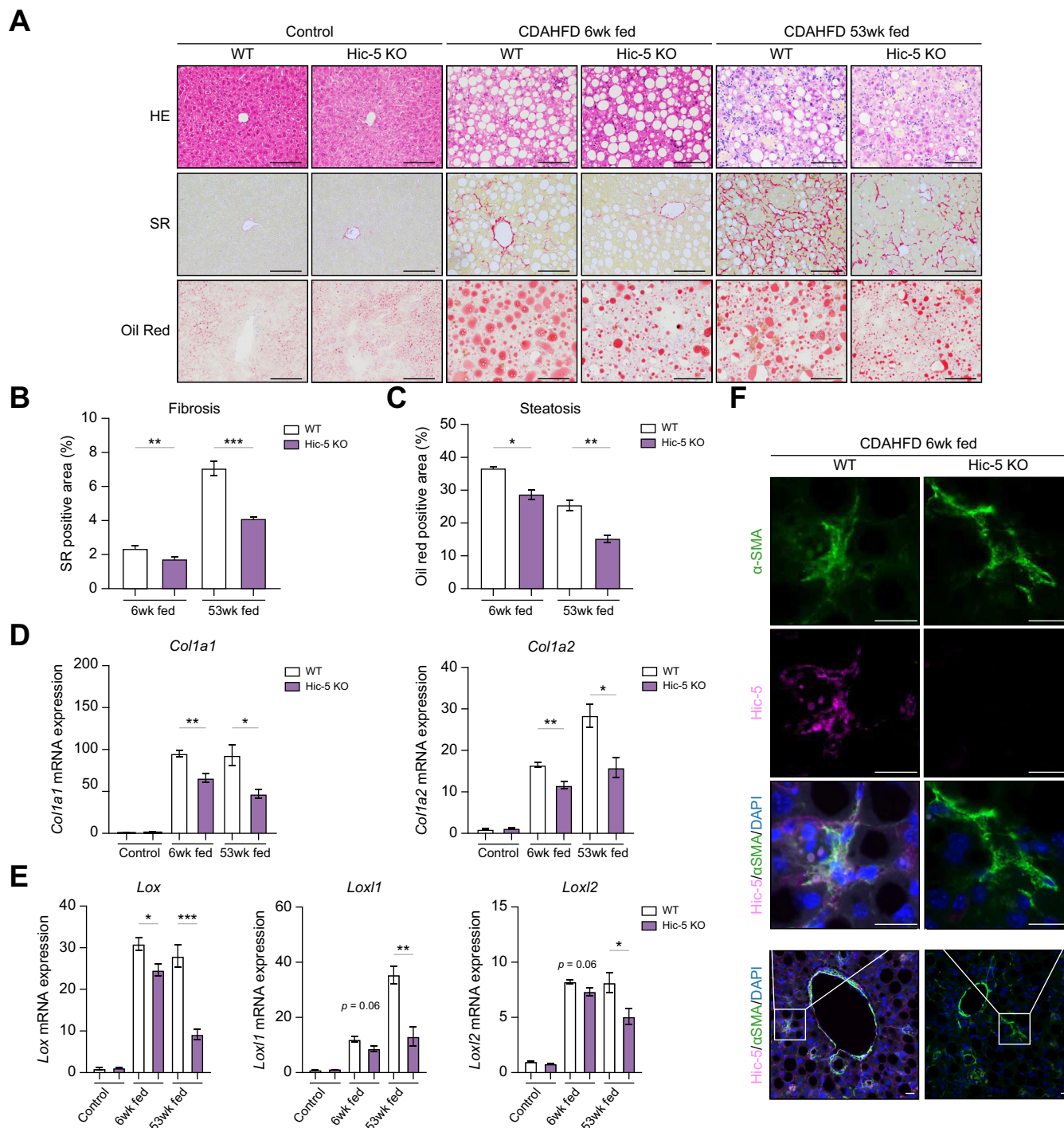
Fig. 4. Hic-5 deletion attenuates fibrosis and steatosis. (A) Representative images of H&E, SR, and Oil Red O staining in livers of mice fed standard chow for 6 weeks (control) or CDAHFD for 3–15 weeks. (B) Quantitation of hepatic fibrosis. Scale bars: 200 μm (n = 4–7/group). (C) Quantitation of steatosis. (D) *Col1a1* and *Col1a2* expression. (E) *Lox*, *Loxl1*, and *Loxl2* expression. (F) Representative immunofluorescence images of Hic-5 (magenta) and α-SMA (green). Nuclei were counterstained with DAPI (blue). Scale bars: 10 μm. Values are mean ± SEM. *p <0.05, **p <0.01, ***p <0.001, two-tailed Student's t test. α-SMA, alpha-smooth muscle actin; CDAHFD, choline-deficient, L-amino acid-defined, high-fat diet; SR, Sirius Red.

Hic-5 expression, which was highly localized to focal adhesions in human HSCs (Fig. 6F), and decreased Hic-5 protein levels (Fig. 6G). To investigate whether anti-*Hic-5* ASOs suppressed Hic-5 expression in mouse livers, we performed gymnosis experiments, which are generally more predictive of *in vivo* ASO uptake, to select the most promising anti-*Hic-5* ASO for *in vivo* experiments. Because only H26 decreased Hic-5 expression after 3 days of transfection (Fig. 6H), H26 was used for *in vivo* experiments. These experiments indicated anti-*Hic-5* ASOs suppressed mRNA expression and protein levels of Hic-5.
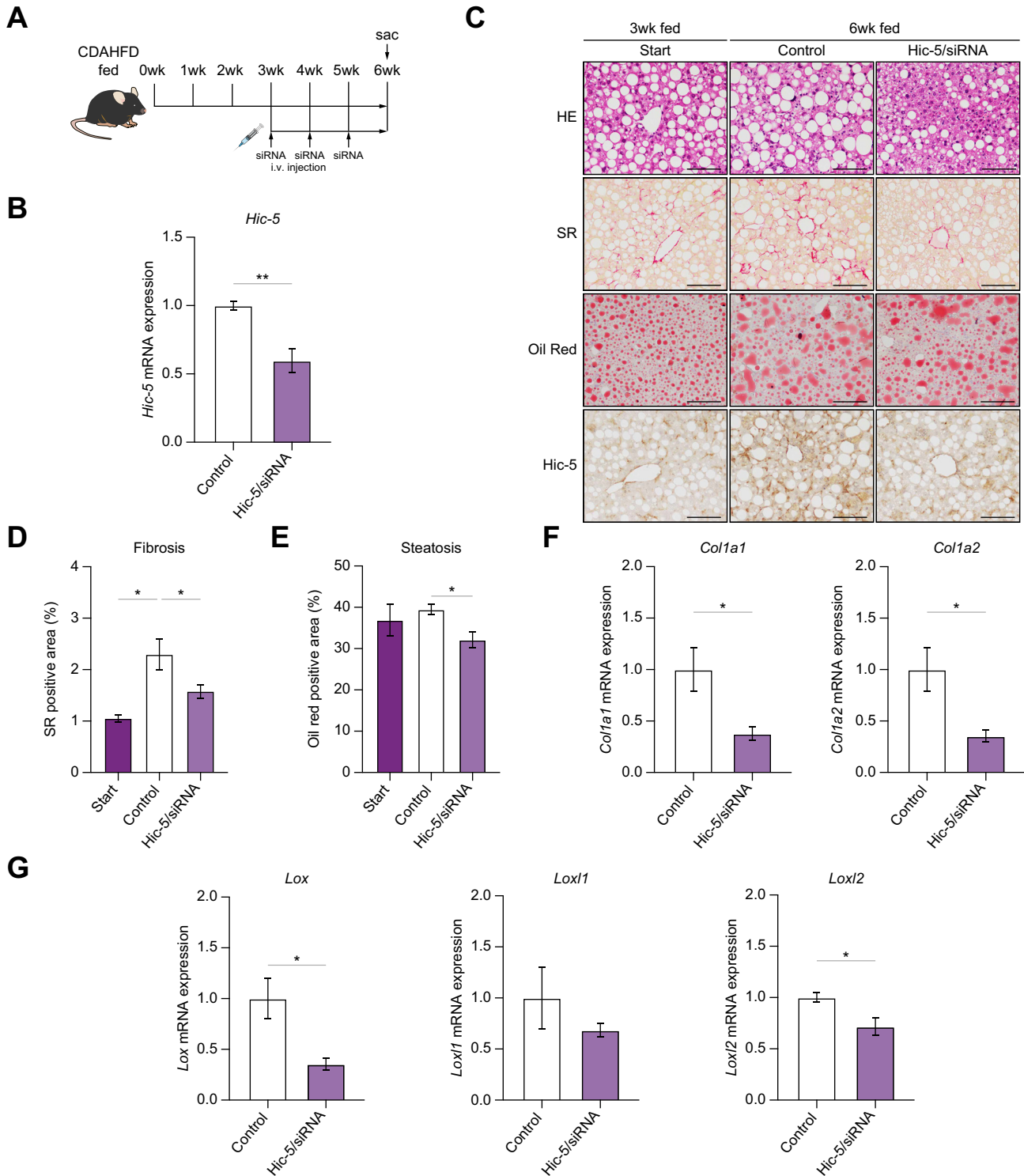
Fig. 5. *In vivo* knockdown of Hic-5 decreases fibrosis and steatosis. (A) Timeline of the experimental procedure (n = 8/group). (B, C) Representative images of HE, SR, and Oil Red O staining in mouse livers. 'Start' indicates baseline at initiation of siRNA administration. Scale bars: 200 μm (n = 3–8/group). Quantitation of (D) hepatic fibrosis and (E) steatosis. (F) *Col1a1* and *Col1a2* expression. (G) *Lox*, *Loxl1*, and *Loxl2* expression. Values are means ± SEM. *p <0.05, **p <0.01, ***p <0.001, two-tailed Student's *t* test. CDAHFD, choline-deficient, L-amino acid-defined, high-fat diet; siRNA, small interfering RNA; SR, Sirius Red.
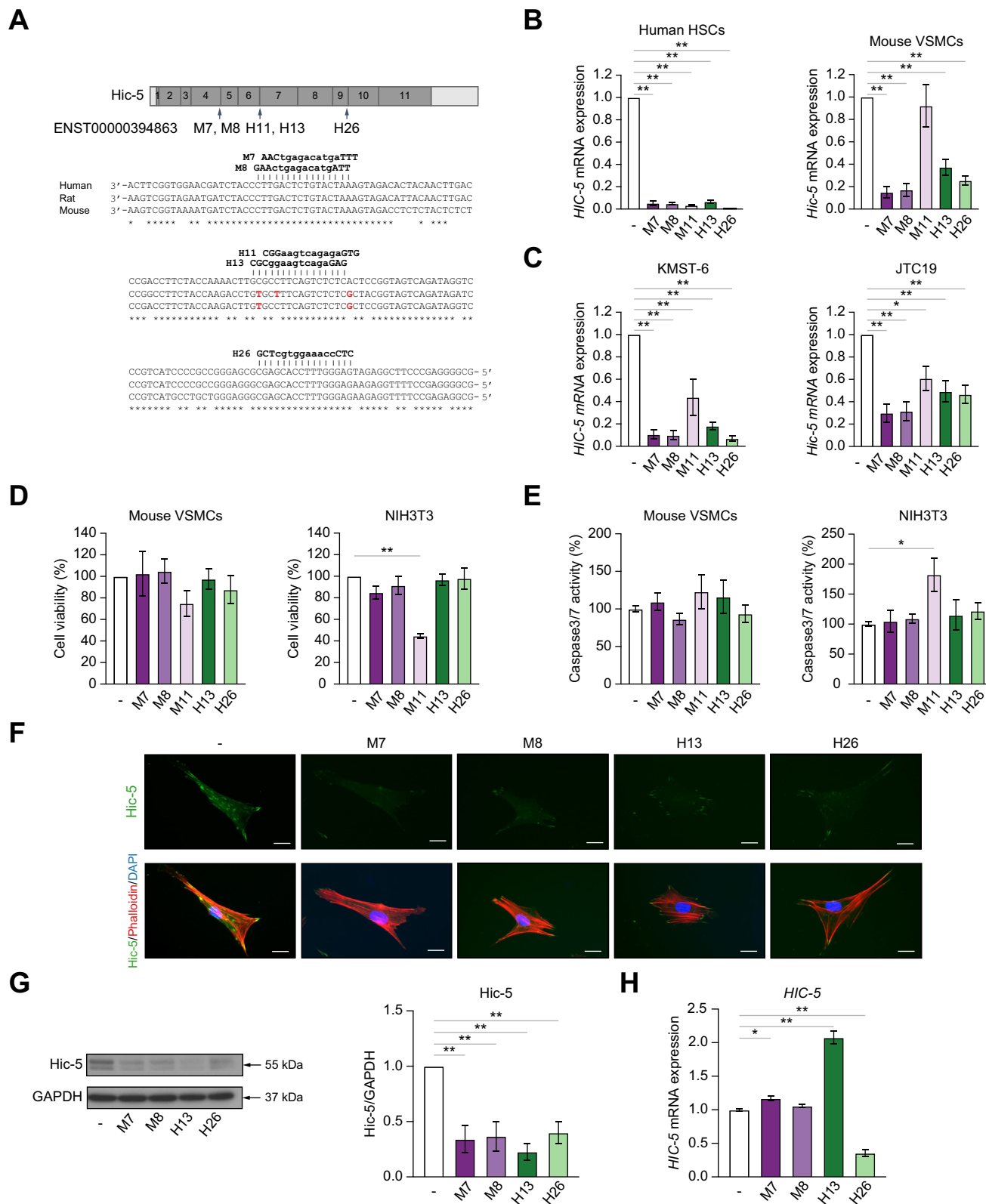
Fig. 6. Activities of anti-*Hic-5* ASOs *in vitro*. (A) Alignment of *Hic-5* mRNA sequences from mammalian genomes. (B, C) Hic-5 mRNA in cells transfected with anti-*Hic-5* ASOs. (-) Control. (D) Cell viability of mouse VSMCs and NIH3T3 cells with ASOs. (E) Caspase 3/7 activation induced by ASOs in mouse VSMCs and NIH3T3 cells. (F) Representative double immunofluorescence images of Hic-5 (green) and phalloidin (red) in human HSCs transfected with anti-*Hic-5* ASOs. (-) Control. Nuclei were counterstained with DAPI (blue). Original magnification: 400 × . Scale bars: 20 μm. (G) Hic-5 protein levels. (H) Gymnosis experiments. Values are mean ± SEM. *p <0.05, **p <0.01, Dunnett's multiple comparison test. ASOs, antisense oligonucleotides; GADPH, glyceraldehyde-3-phosphate dehydrogenase; HSCs, hepatic stellate cells; VSMCs, vascular smooth muscle cells.
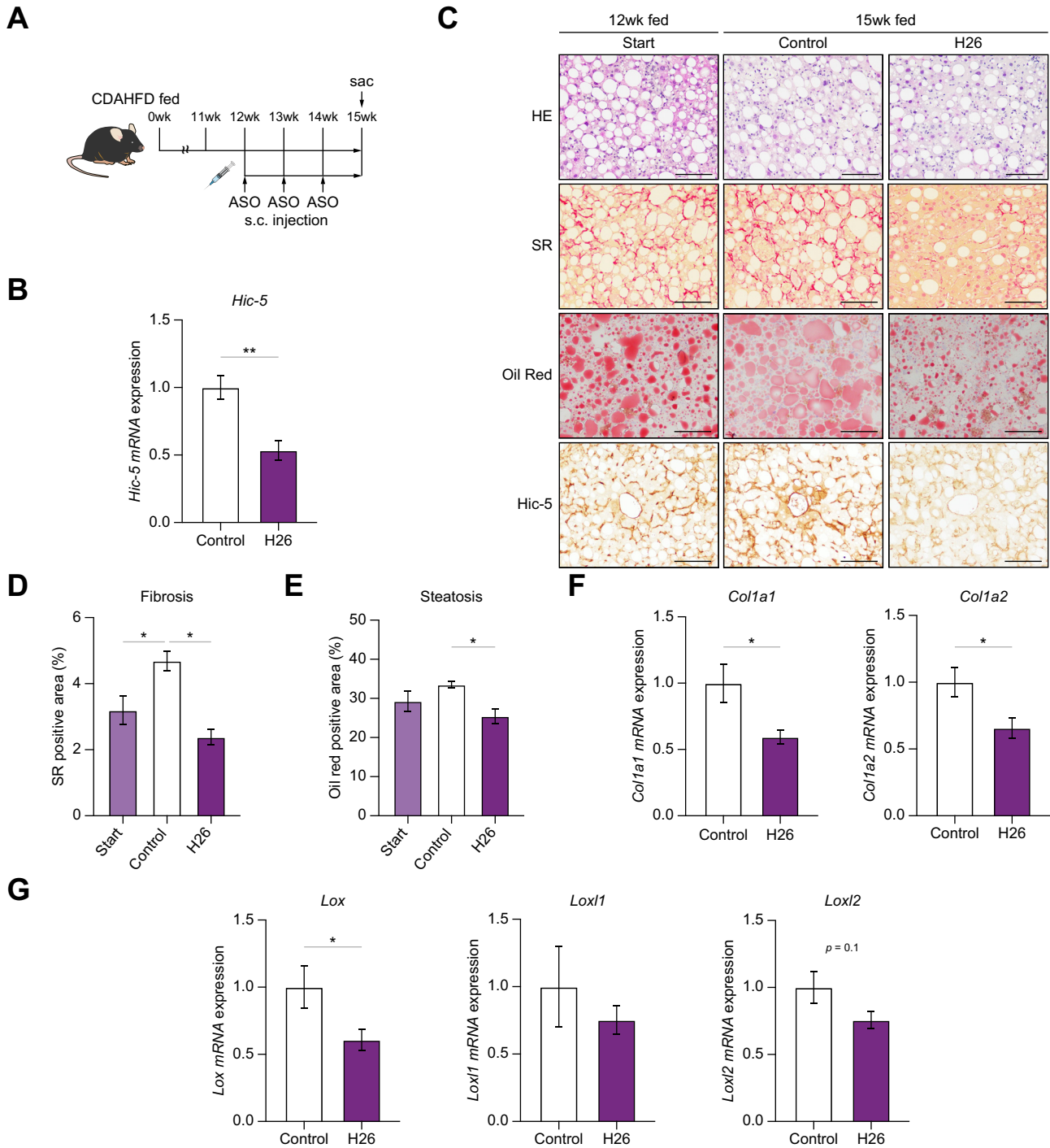
Fig. 7. Anti-*Hic-5* ASO attenuates advanced fibrosis and steatosis. (A) Timeline of the experimental procedure (*n* = 6/group). (B, C) Representative images of HE, SR, and Oil Red O staining in mouse livers. 'Start' indicates baseline at initiation of ASO administration. Scale bars: 200 μm (*n* = 6/group). (D) Quantitation of hepatic fibrosis. (E) Quantitation of steatosis. (F) *Col1a1* and *Col1a2* expression. (G) *Lox*, *Loxl1*, and *Loxl2* expression. Values are mean ± SEM. **p* <0.05, ***p* <0.01, two-tailed Student's *t* test. ASOs, antisense oligonucleotides; CDAHFD, choline-deficient, L-amino acid-defined, high-fat diet; SR, Sirius Red.

Anti-*Hic-5* ASO attenuates advanced fibrosis and steatosis in a MASH model

To assess the therapeutic potential of anti-*Hic*-5 ASO to prevent advanced fibrosis in the MASH model, the subcutaneous administration of H26 was performed once a week for 3 weeks following 12 weeks of CDAHFD ([Fig. 7](#)A). Mice were sacrificed 1 week after the final ASO administration (15th week of CDAHFD). H26-treated mice had significantly lower *Hic-5*

mRNA expression and significantly less hepatic steatosis and fibrosis compared with controls (Fig. 7B–E). No macroscopic changes in livers were observed (Fig. S4C). Liver injury, assessed by measuring blood AST and ALT, was not significantly changed in the H26-injected group (Fig. S5B). However, AST levels tended to be suppressed in H26-treated mice. *Col1a1, Col1a2,* and *Lox* mRNA expressions were significantly lower in H26-treated mice compared with controls (Fig. 7F and G).

Discussion

This study reports Hic-5 is a mediator of advanced fibrosis and is a promising therapeutic target for MASH. Initially, Hic-5 was thought to mediate fibrotic processes in MASLD.[10,23] However, we demonstrated the potential of Hic-5 to modulate steatosis. Indeed, human hepatic Hic-5 was upregulated during MASLD progression, particularly in cases with advanced fibrosis. Furthermore, our murine model results strongly suggest that mitigation of the pathological state in MASH-afflicted livers can be achieved by inhibiting Hic-5.

The coefficient of determination R^2 applied to histopathological human tissue analysis predicts 3,3′-diaminobenzidine image quantification accurately, demonstrating good predictive capabilities. However, its accuracy was not as satisfactory for fluorescence image analysis because it was performed using fields selected to avoid autofluorescence. Nevertheless, positive area image analysis and fluorescence image analysis demonstrated similar correlation trends, indicating consistent findings for both methods. In the public data analysis, Hic-5 and collagen type 1 gene expressions were positively correlated between the two datasets, although R^2 was low owing to sampling conditions. HSC proportions within the liver assessed by scRNA-seq analysis were low and HSC cell populations were absent in some samples potentially related to variations in facility sampling and specimen collection methods. Hic-5 is predominantly expressed in HSCs suggesting these influences contributed to a lower R^2 value. However, in a MASH model, a significantly high R^2 was obtained for the comparison between Hic-5 and collagen expressions, suggesting careful attention to sampling conditions of human specimens might achieve similar results. Human liver samples used in this study predominantly consisted of non-MASH specimens. Consequently, we intend to explore further the association between intrahepatic Hic-5 expression and human MASH.

HSCs play a crucial role in liver fibrosis by producing collagen and elastic fibers. Previous studies reported Hic-5 is prominent in HSCs and its expression increased during cell activation.[10] Naked ASO can be delivered to non-parenchymal cells, including HSCs.[24] However, there are currently no nucleic acids selectively target HSCs, although a conjugated ASO targeting hepatocyte-like N-galactosamine. Future studies will develop ASOs with improved delivery efficiency to HSCs.

Conventional drug targets include growth factors and cytokines, and their associated receptors and kinases.[25,26] Although drug discovery aimed at adaptor molecules lacking enzymatic activity was considered a significant challenge,[26,27] the development of innovative drug candidates targeting these molecules has become possible.[27–30] Of these, ASOs stand out, with several approved nucleic acid drugs already demonstrating therapeutic efficacy against genetic disorders.[28,31] Given the hepatic translocation capability of ASOs, our elucidation of their mechanisms

will aid the development of new therapeutic strategies to treat MASLD and advanced fibrosis.

The present study investigated anti-*Hic-5* ASOs as therapeutic agents for advanced liver fibrosis. Four of the designed anti-*Hic-5* ASOs suppressed *Hic-5* mRNA expression in human, murine, and rat cells with low cytotoxicity. Anti-*Hic-5* ASOs M8, H13, and H26 decreased protein levels of α-SMA and Col1a1, markers of activated HSCs that are increased in liver fibrosis. *In vivo* experiments showed multiple injections of H26 suppressed the expressions of *Hic-5, Col1a1, Col1a2,* and *Lox*, which are fibrosis-related genes in mouse livers, resulting in a smaller liver fibrosis area. Collectively, these results suggest H26 is a potential therapeutic agent for advanced hepatic fibrosis. Moreover, we showed anti-*Hic-5* ASOs mitigated hepatic steatosis despite Hic-5 being predominantly expressed in non-parenchymal cells, particularly HSCs. The underlying mechanism by which Hic-5 mediates steatosis warrants further investigation.

After intravenous administration, naked siRNA undergoes rapid degradation by nucleases in the bloodstream. For siRNA experiments, Invivofectamine 3.0 (invitrogen, Carlsbad, CA) was used for *in vivo* transfection as previously described.[32,33] For ASO, phosphorothioate and LNA modifications were incorporated into nucleic acids to enhance stability against degradation and promote binding to plasma proteins.[34] Thus, naked ASO was used for *in vivo* ASO treatment experiments.

We previously used Hic-5 siRNA to show Hic-5 is a therapeutic target for liver fibrosis.[10] Here, we developed anti-*Hic-5* ASOs and assessed their therapeutic efficacy for treating advanced liver fibrosis and steatosis. Although ASOs and siRNAs have been used as therapeutic agents, ASOs are easily delivered to the liver. Hic-5 has emerged as a promising therapeutic target for a spectrum of diseases—Hic-5 deficiency mitigated liver fibrosis and had a positive effect on pancreatic fibrosis, abdominal aortic aneurysms, colorectal cancer, and osteoarthritis, all of which involve ECM remodeling.[21,23,35,36] We previously demonstrated Hic-5 siRNA attenuated rat surgically-induced osteoarthritis.[37] Because H26 is a therapeutic candidate for multiple diseases, the development of an effective system for delivering ASOs to organs other than the liver and kidney and defining the most suitable route of administration is necessary.

We previously reported Hic-5 modulated Smad2 phosphorylation via Smad7, downstream of the TGF-β signaling pathway.[10] Here, we showed that H26 mitigated advanced liver fibrosis by inhibiting *Lox* expression. LOX enzymes that crosslink collagen and elastin promote the progression of fibrosis by fostering a rigid matrix.[38–43] Furthermore, LOX and LOXL2 expressions were increased in fibrotic livers of patients with Wilson's disease and primary biliary cirrhosis.[18] A phase II clinical trial to ameliorate liver fibrosis by simtuzumab, a monoclonal antibody targeting LOXL2, in patients with liver fibrosis reported poor clinical benefit;[40,44,45] it only achieved a 50% inhibition of enzymatic activity *in vitro* owing to its indirect and allosteric mechanism of action,[19] and was selective for LOXL2 rather than all LOX isoforms, despite crosstalk between LOX family members during fibrosis.

In contrast, H26 reduced *Col1a1* and *Col1a2* expressions, LOX family member substrates and constituents of the fibrotic ECM. Furthermore, H26 significantly reduced *Lox* expression in fibrotic mouse livers and tended to reduce *Loxl1* and *Loxl2*

expressions. Thus, H26 may have superior antifibrotic efficacy compared with simtuzumab.

Recent applications of modified nucleic acid technology to antisense nucleic acid drug development have enhanced the *in vivo* stability and membrane permeability of ASOs, facilitating systemic administration without the need for a carrier. Furthermore, the development of conjugates harnessing this technology promises to extend the application of H26 beyond liver fibrosis to include steatosis and other diseases.

This study had several limitations. First, the mechanistic role of Hic-5 in steatosis remains to be investigated. Second, additional factors might contribute to the pathogenesis of advanced fibrosis in MASH. Future research should investigate downstream signaling pathways involving Hic-5. Third, CDAHFD model mice yielded results specific to choline and methionine metabolism-related MASH pathogenesis. Therefore, we plan to analyze the pathological control ability of Hic-5, especially for steatosis, using other MASH model mice to achieve a condition closer to that of humans. Last, although we established an association between Hic-5 expression and the progression of MASH with fibrosis in patients, intervention studies were conducted in mice. Therefore, the translational relevance of H26 in human MASH and fibrosis is imperative. Nonetheless, our study underscores the potential of Hic-5 inhibition as an innovative therapeutic strategy for advanced fibrosis and MASLD.

Affiliations

[1]*Department of Biochemistry, Showa University School of Medicine; Shinagawa-ku, Tokyo, Japan;* [2]*Institute for Extracellular Matrix Research, Showa University; Shinagawa-ku, Tokyo, Japan;* [3]*Department of Life Science and Technology, Tokyo Institute of Technology; Yokohama, Kanagawa, Japan;* [4]*Division of Gastroenterology, Department of Medicine, Showa University School of Medicine; Shinagawa-ku, Tokyo, Japan;* [5]*Department of Dermatology, Showa University School of Medicine; Shinagawa-ku, Tokyo, Japan;* [6]*Department of General and Gastroenterological Surgery, Showa University School of Medicine; Shinagawa-ku, Tokyo, Japan*

Abbreviations

α-SMA, alpha-smooth muscle actin; ALT, alanine aminotransferase; ASO, antisense oligonucleotide; AST, aspartate aminotransferase; CDAHFD, choline-deficient L-amino acid-defined high-fat diet; ECM, extracellular matrix; GADPH, glyceraldehyde-3-phosphate dehydrogenase; Hic-5, hydrogen peroxide-inducible clone-5; HSCs, hepatic stellate cells; KO, knockout; LNAs, locked nucleic acids; LOX, lysyl oxidase; MASLD, metabolic dysfunction-associated steatotic liver disease; MASH, metabolic dysfunction-associated steatohepatitis; qPCR, quantitative real-time reverse transcriptase PCR; Iba1, ionized calcium-binding adaptor molecule 1; scRNA-seq, single-cell RNA sequencing; siRNA, small interfering RNA; SMCs, smooth muscle cells; SR, Sirius Red; TGF, transforming growth factor; VSMCs, vascular smooth muscle cells; WT, wild type.

Conflicts of interest

The authors declare no competing interests.

Please refer to the accompanying ICMJE disclosure forms for further details.

Authors' contributions

Conceived and designed the experiments: JKK, KS. Performed all animal experiments and analyzed the data: MN, AyM, MKT. Conducted *in vitro* experiments: AyM. Analysis of *in vitro* experiments: JKK, YM. Design and synthesis of antisense oligonucleotides: KS, YM. Conducted the human sample experiments and analyzed the data: M.S., AkM, HY, TA. Designed the figures and wrote the manuscript: JKK, MN, AyM. Approved the final version of the manuscript: all authors.

Data availability statement

Data analyzed in this study are available upon reasonable request.

Supplementary data

Supplementary data to this article can be found online at https://doi.org/10.1016/j.jhepr.2024.101195.

References

Author names in bold designate shared co-first authorship

[1] **Wong VW-S, Ekstedt M**, Wong GL-H, et al. Changing epidemiology, global trends and implications for outcomes of NAFLD. J Hepatol 2023;79:842–852.

[2] **Hagström H, Nasr P**, Ekstedt M, et al. Fibrosis stage but not NASH predicts mortality and time to development of severe liver disease in biopsy-proven NAFLD. J Hepatol 2017;67:1265–1273.

[3] Friedman SL. Mechanisms of hepatic fibrogenesis. Gastroenterology 2008;134:1655–1669.

[4] Mao Y, Yu F, Wang J, et al. Autophagy: a new target for nonalcoholic fatty liver disease therapy. Hepat Med 2016;8:27–37.

[5] Hirschfield GM, Dyson JK, Alexander GJM, et al. The British Society of Gastroenterology/UK-PBC primary biliary cholangitis treatment and management guidelines. Gut 2018;67:1568–1594.

[6] Sun M, Kisseleva T. Reversibility of liver fibrosis. Clin Res Hepatol Gastroenterol 2015;39:S60–S63.

[7] Lee UE, Friedman SL. Mechanisms of hepatic fibrogenesis. Best Pract Res Clin Gastroenterol 2011;25:195–206.

[8] Shibanuma M, Mashimo J, Kuroki T, et al. Characterization of the TGF beta 1-inducible hic-5 gene that encodes a putative novel zinc finger protein and its possible involvement in cellular senescence. J Biol Chem 1994;269:26767–26774.

[9] **Yao S, Tu Z**, Yang X, et al. Physiological and pathological roles of Hic-5 in several organs. (Review) Int J Mol Med 2022;50:138.

[10] **Lei X-F, Fu W**, Kim-Kaneyama J, et al. Hic-5 deficiency attenuates the activation of hepatic stellate cells and liver fibrosis through upregulation of Smad7 in mice. J Hepatol 2016;64:110–117.

[11] Seki E, Brenner DA. Recent advancement of molecular mechanisms of liver fibrosis. J Hepatobiliary Pancreat Sci 2015;22:512–518.

[12] **Kim-Kaneyama J, Takeda N**, Sasai A, et al. Hic-5 deficiency enhances mechanosensitive apoptosis and modulates vascular remodeling. J Mol Cel Cardiol 2011;50:77–86.

[13] **Pantano L, Agyapong G, Shen Y**, et al. Molecular characterization and cell type composition deconvolution of fibrosis in NAFLD. Sci Rep 2021;11:18045.

[14] **Kozumi K, Kodama T, Murai H**, et al. Transcriptomics identify thrombospondin-2 as a biomarker for NASH and advanced liver fibrosis. Hepatology 2021;74:2452–2466.

[15] Love MI, Huber W, Anders S. Moderated estimation of fold change and dispersion for RNA-seq data with DESeq2. Genome Biol 2014;15:550.

[16] Matsumoto M, Hada N, Sakamaki Y, et al. An improved mouse model that rapidly develops fibrosis in non-alcoholic steatohepatitis. Int J Exp Path 2013;94:93–103.

[17] Kagan HM. Lysyl oxidase: mechanism, regulation and relationship to liver fibrosis. Pathol Res Pract 1994;190:910–919.

[18] Vadasz Z, Kessler O, Akiri G, et al. Abnormal deposition of collagen around hepatocytes in Wilson's disease is associated with hepatocyte specific expression of lysyl oxidase and lysyl oxidase like protein-2. J Hepatol 2005;43:499–507.

[19] Barry-Hamilton V, Spangler R, Marshall D, et al. Allosteric inhibition of lysyl oxidase–like-2 impedes the development of a pathologic microenvironment. Nat Med 2010;16:1009–1017.

[20] Perepelyuk M, Terajima M, Wang AY, et al. Hepatic stellate cells and portal fibroblasts are the major cellular sources of collagens and lysyl oxidases in normal liver and early after injury. Am J Physiol Gastrointest Liver Physiol 2013;304:G605–G614.

[21] Omoto T, Kim-Kaneyama J, Lei X-F, et al. The impact of stromal Hic-5 on the tumorigenesis of colorectal cancer through lysyl oxidase induction and stromal remodeling. Oncogene 2018;37:1205–1219.

[22] Zuker M. Mfold web server for nucleic acid folding and hybridization prediction. Nucleic Acids Res 2003;31:3406–3415.

[23] Gao L, Lei X-F, Miyauchi A, et al. Hic-5 is required for activation of pancreatic stellate cells and development of pancreatic fibrosis in chronic pancreatitis. Sci Rep 2020;10:19105.

[24] Watanabe A, Nakajima M, Kasuya T, et al. Comparative characterization of hepatic distribution and mRNA reduction of antisense oligonucleotides conjugated with triantennary N-acetyl galactosamine and lipophilic ligands targeting apolipoprotein B. J Pharmacol Exp Ther 2016;357:320–330.

[25] Schwartz DM, Kanno Y, Villarino A, et al. JAK inhibition as a therapeutic strategy for immune and inflammatory diseases. Nat Rev Drug Discov 2017;16:843–862.

[26] Cohen P, Cross D, Jänne PA. Kinase drug discovery 20 years after imatinib: progress and future directions. Nat Rev Drug Discov 2021;20:551–569.

[27] Kulkarni JA, Witzigmann D, Thomson SB, et al. The current landscape of nucleic acid therapeutics. Nat Nanotechnol 2021;16:630–643.

[28] Egli M, Manoharan M. Chemistry, structure and function of approved oligonucleotide therapeutics. Nucleic Acids Res 2023;51:2529–2573.

[29] Zhang Z, Conniot J, Amorim J, et al. Nucleic acid-based therapy for brain cancer: challenges and strategies. J Control Release 2022;350:80–92.

[30] Sridharan K, Gogtay NJ. Therapeutic nucleic acids: current clinical status. Br J Clin Pharmacol 2016;82:659–672.

[31] Hill SF, Meisler MH. Antisense oligonucleotide therapy for neuro-developmental disorders. Dev Neurosci 2021;43:247–252.

[32] Eguchi A, De Mollerat Du Jeu X, Johnson CD, et al. Liver Bid suppression for treatment of fibrosis associated with non-alcoholic steatohepatitis. J Hepatol 2016;64:699–707.

[33] Morton RE, Liu Y, Izem L. ApoF knockdown increases cholesteryl ester transfer to LDL and impairs cholesterol clearance in fat-fed hamsters. J Lipid Res 2019;60:1868–1879.

[34] Swayze EE, Siwkowski AM, Wancewicz EV, et al. Antisense oligonucleotides containing locked nucleic acid improve potency but cause significant hepatotoxicity in animals. Nucleic Acids Res 2007;35:687–700.

[35] Lei X, Kim-Kaneyama J, Arita-Okubo S, et al. Identification of Hic–5 as a novel scaffold for the MKK4/p54 JNK pathway in the development of abdominal aortic aneurysms. J Am Heart Assoc 2014;3:e000747.

[36] Miyauchi A, Kim-Kaneyama J, Lei X-F, et al. Alleviation of murine osteoarthritis by deletion of the focal adhesion mechanosensitive adapter, Hic-5. Sci Rep 2019;9:15770.

[37] Miyauchi A, Noguchi M, Lei X-F, et al. Knockdown of mechanosensitive adaptor Hic-5 ameliorates post-traumatic osteoarthritis in rats through repression of MMP-13. Sci Rep 2023;13:7446.

[38] Zhao W, Yang A, Chen W, et al. Inhibition of lysyl oxidase-like 1 (LOXL1) expression arrests liver fibrosis progression in cirrhosis by reducing elastin crosslinking. Biochim Biophys Acta Mol Basis Dis 2018;1864:1129–1137.

[39] Liu SB, Ikenaga N, Peng Z, et al. Lysyl oxidase activity contributes to collagen stabilization during liver fibrosis progression and limits spontaneous fibrosis reversal in mice. FASEB J 2016;30:1599–1609.

[40] Ikenaga N, Peng Z-W, Vaid KA, et al. Selective targeting of lysyl oxidase-like 2 (LOXL2) suppresses hepatic fibrosis progression and accelerates its reversal. Gut 2017;66:1697–1708.

[41] Harlow CR, Wu X, Van Deemter M, et al. Targeting lysyl oxidase reduces peritoneal fibrosis. PLoS ONE 2017;12:e0183013.

[42] Dongiovanni P, Meroni M, Baselli GA, et al. Insulin resistance promotes Lysyl Oxidase like 2 induction and fibrosis accumulation in non-alcoholic fatty liver disease. Clin Sci (Lond) 2017;131:1301–1315.

[43] Aumiller V, Strobel B, Romeike M, et al. Comparative analysis of lysyl oxidase (like) family members in pulmonary fibrosis. Sci Rep 2017;7:149.

[44] Meyer KC. Great expectations for simtuzumab in IPF fall short. Lancet Respir Med 2017;5:2–3.

[45] Fickert P. Is this the last requiem for simtuzumab? Hepatology 2019;69:476–479.